JOC*Article*

Mechanistic Studies on the Stereoselective Formation of β-Mannosides from Mannosyl Iodides Using α-Deuterium Kinetic Isotope Effects

Mohamed H. El-Badri, Dan Willenbring, Dean J. Tantillo,* and Jacquelyn Gervay-Hague*

University of California, Davis, Department of Chemistry, One Shields Avenue, Davis, California 95616

gervay@chem.ucdavis.edu; tantillo@chem.ucdavis.edu

Received February 2, 2007

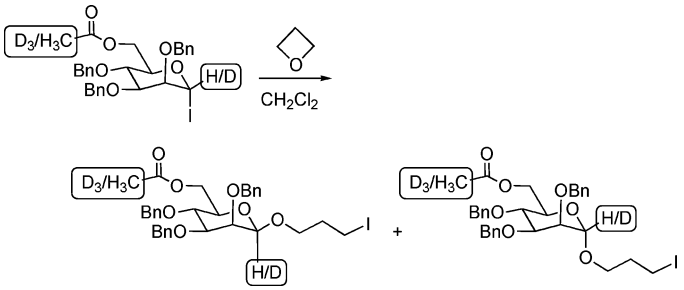

Stereoselective synthesis of β-mannosides is one of the most challenging linkages to achieve in carbohydrate chemistry. Both the anomeric effect and the C2 axial substituent favor the formation of the axial glycoside (α-product). Herein, we describe mechanistic studies on the β-selective glycosidation of trimethylene oxide (TMO) using mannosyl iodides. Density functional calculations (at the B3LYP/6-31+G(d,p):LANL2DZ level) suggest that formation of both α- and β-mannosides involve loose S_N2-like transition-state structures with significant oxacarbenium character, although the transition structure for formation of the α-mannoside is significantly looser. α-Deuterium kinetic isotope effects (α-DKIEs) based upon these computed transition state geometries match reasonably well with the experimentally measured values: 1.16 ± 0.02 for the β-linkage (computed to be 1.15) and 1.19 ± 0.05, see table 2 for the α-analogue (computed to be 1.26). Since it was unclear if β-selectivity resulted from a conformational constraint induced by the anomeric iodide, a 4,6-*O*-benzylidine acetal was used to lock the iodide into a chairlike conformation. Both experiments and calculations on this analogue suggest that it does not mirror the behavior of mannosyl iodides lacking bridging acetal protecting groups.

Introduction

β-Mannosides are major constituents in many biologically important structures,[1−5] and numerous efforts have focused on synthesizing mannoside linkages with high β-selectivity.[6−16] Typically, a suitably protected electrophilic mannose analogue possessing a leaving group at the anomeric center serves as a glycosyl donor and reacts with a nucleophilic oxygen of an acceptor. There remains a need for more effective, easily prepared mannosyl donors that allow for the formation of β-mannosides in high yields and good stereoselectivity with a variety of acceptors. Our efforts in this direction have focused on the use of glycosyl iodides.[17−21] Our previous observation that THF, but not diethyl ether, acts as a capable acceptor

(1) Paulsen, H. *Angew. Chem., Int. Ed. Engl.* **1982**, *21*, 155−173.
(2) Lam, S. N.; Gervay-Hague, J. *J. Org. Chem.* **2005**, *70*, 8772 -8779.
(3) Crich, D.; Banerjee, A.; Yao, Q. *J. Am. Chem. Soc.* **2004**, *126*, 14930−14934.
(4) Joshi, H.; Kapoor, V. P. *Carbohydr. Res.* **2003**, *338*, 1907−1912.
(5) Gridley, J. J.; Osborn, H. M. I. *J. Chem. Soc., Perkin Trans. 1* **2000**, 1471−1791.
(6) Paulsen, H.; Lokhoff, O. *Chem. Ber.* **1981**, *114*, 3102−3114.
(7) Sirivastava, V. K.; Schuerch, C. *J. Org. Chem.* **1981**, *46*, 1121−1126.
(8) Barresi, F.; Hindsgaul, O. *J. Am. Chem. Soc.* **1991**, *113*, 9376−9377.
(9) Barresi, F.; Hindsgaul, O. *Synlett* **1992**, 759−761.
(10) Stork, G.; Kim, G. *J. Am. Chem. Soc.* **1992**, *114*, 1087−1088.
(11) Kunz, H.; Gunther, W. *Angew. Chem., Int. Ed. Engl.* **1988**, *27*, 1086−1087.
(12) Crich, D.; Sun, S. *J. Am. Chem. Soc.* **1997**, *119*, 11217−11223.
(13) Crich, D.; Smith, M. *J. Am. Chem. Soc.* **2001**, *123*, 9015−9020.
(14) Hodosi, G.; Kovac, P. *J. Am. Chem. Soc.* **1997**, *119*, 2335−2336.
(15) Kim, W.-S.; Sasai, H.; Shibasaki, M. *J. Org. Chem.* **1995**, *60*, 4−5.
(16) Toshima, K.; Kasumi, K.-I.; Matsumura, S. *Synlett* **1998**, 643−645.
(17) Lam, S. N.; Gervay-Hague, J. *Org. Lett.* **2002**, *4*, 2039−2042.

10.1021/jo070229y CCC: $37.00
Published on Web 06/01/2007

SCHEME 1. Mannosylation Reaction of Iodide 1 with TMO under Neutral Conditions

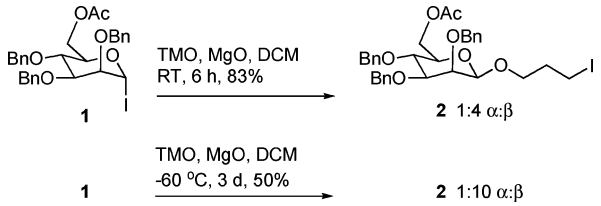

SCHEME 2. Synthesis and Glycosylation Reaction of 6-*O*-PNB Mannosyl Iodide

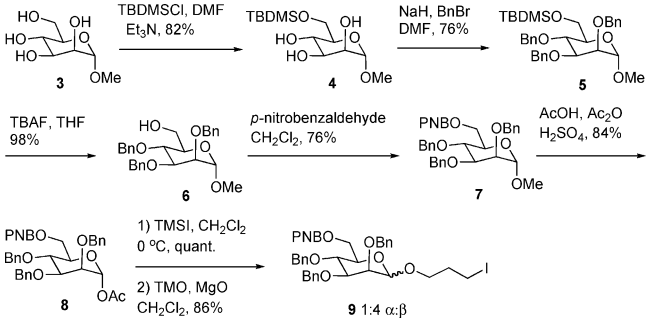

inspired us to investigate the reactivity of a variety of cyclic ethers with glycosyl iodides.[22] Preliminary studies in this area showed that reactions with strained cyclic oxa- and thioethers proceeded under neutral conditions yielding the corresponding glycosides in excellent yields and with high β-selectivity.[22]

Of the acceptors explored so far, we are particularly interested in trimethylene oxide (TMO) because of its potential versatility in natural product synthesis.[23,24] A representative reaction using TMO is shown in Scheme 1. Mannosyl iodide **1**, possesses an acetate group at the O-6 position, which attenuates the reactivity of the iodide giving greater stereocontrol.[22] The reaction of TMO with **1** produces mannosides **2** with 4:1 β-selectivity at room temperature,[22] and up to 10:1 β-selectivity at lower temperatures.[25] With the ultimate goal of increasing this selectivity, we set out to examine the mechanism for this reaction.

To rule out the possibility that the acyl group at C6 is participating in these substitution reactions,[26,27] we replaced this acetyl group with a *p*-nitrobenzyl (PNB) group, a "disarming" functionality that lacks the ability to directly interact with the anomeric carbon. The synthesis of this analogue (**8**) is shown in Scheme 2. Selective protection of the O-6 hydroxyl group in mannoside **3** was accomplished using *tert*-butyldimethylsilyl chloride in dimethylformamide to afford compound **4** in 82% yield.[28] Benzylation of **4** yielded the fully protected methyl mannoside **5** in 76% yield. Deprotection of the silyl protecting group using tetrabutylammonium fluoride delivered **6** in quantitative yield,[29] and subsequent *p*-nitrobenzylation of **6**[30] followed by acetylation at the anomeric center[31] afforded mannosyl acetate **8** in 64% yield over two steps.

SCHEME 3. Synthesis of 1-Deuteromannose Diol

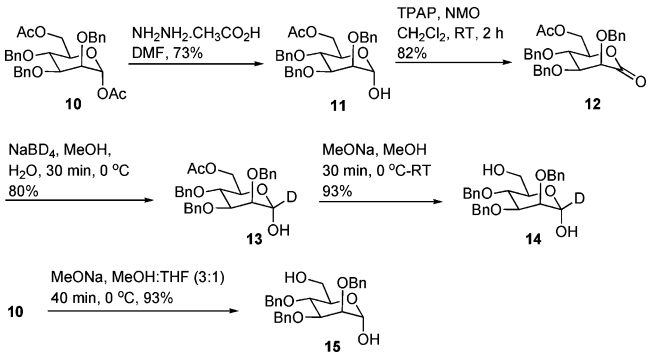

We were now set to explore the effects of switching the *O*-6-acetyl group for an *O*-6-PNB group on the TMO reaction. Generation of the corresponding mannosyl iodide from **8** followed by reaction with TMO yielded mannosides **9** (86% over two steps; Scheme 2). Upon characterization of the anomeric ratio for these compounds, we found that the mannosyl iodide bearing an *O*-6-PNB group displayed the same reactivity and stereoselectivity observed for the *O*-6-acetyl analog, Scheme 1, indicating that participation of the C-6 acetate is not a competing factor in these reactions.

Previously,[25] we suggested that the β-mannoside arises from nucleophilic displacement of the α-iodide in an S_N2-like fashion, while the α-mannoside results from either attack on an oxacarbenium intermediate or from direct displacement of the β-glycosyl iodide generated from in situ anomerization, Figure 1.[32] We now describe additional experiments and quantum chemical calculations aimed at testing the validity of these hypotheses.

Results and Discussion

First, we undertook the experimental determination of the α-deuterium kinetic isotope effects (α-DKIEs, k_H/k_D) for the transformation described in Scheme 1. Our approach was based on studies previously described by Crich and co-workers of β-mannoside formation using labeled mannosyl triflates.[33] Crich's experiment, along with other previous work, suggested that very small α-DKIEs ($k_H/k_D \sim 1.0-1.1$) are consistent with S_N2-like processes with relatively tight transition state structures, while larger α-DKIEs ($k_H/k_D \sim 1.1-1.4$) are consistent with rate-determining transition state structures with significant oxacarbenium ion character (i.e., S_N1 or S_N2 processes with loose transition-state structures).[34,35] Our synthesis of compound

(18) Lam, S. N.; Gervay-Hague, J. *Carbohydr. Res.* **2002**, *337*, 1953−1965.
(19) Bhat, A. S.; Gervay-Hague, J. *Org. Lett.* **2001**, *3*, 2081−2084.
(20) Gervay, J. *Org. Synth: Theory Appl.* **1998**, *4*, 121−153.
(21) Hadd, M. J.; Gervay, J. *Carbohydr. Res.* **1999**, *320*, 61−69.
(22) Dabideen, D. R.; Gervay-Hague, J. *Org. Lett.* **2004**, *6*, 973−975.
(23) Proemmela, S.; Wartchowb, R.; Hoffmann, H. M. R. *Tetrahedron* **2002**, *58*, 6199−6206.
(24) Hamberg, M.; Svensson, J.; Samuelsson, B. *Proc. Natl. Acad. Sci. U.S.A.* **1975**, *72*, 2994−2998.
(25) El-Badry, M. H.; Gervay-Hague, J. *Tetrahedron Lett.* **2005**, *46*, 6727−6728.
(26) Lin, C.-C.; Shimazaki, M.; Heck, M.; Aoki, S.; Wang, R.; Kimura, T.; Ritzen, H.; Takayama, S.; Wu, S.; Weitz-Schmidt, G.; Wong, C. H. *J. Am. Chem. Soc.* **1996**, *118*, 6826−6840.
(27) Lu, L.-D.; Shie, C.-R.; Kulkarni, S. S.; Pan, G.-R.; Lu, X.-A.; Hung, S.-C. *Org. Lett.* **2006**, *8*, 5995−5998.
(28) Hernandez, O.; Chaudhary, S. K. *Tetrahedron Lett.* **1979**, 95−98.
(29) Corey, E. J.; Venkateswalu, A. *J. Am. Chem. Soc.* **1972**, *94*, 6190.
(30) Izumi, M.; Fukase, K. *Chem. Lett.* **2005**, *34*, 594−595.
(31) Morteza, M. V.; Bernacki, R. J.; Dalley, N. K.; Wilson, B.; Robins, R. *J. Med. Chem.* **1987**, *30*, 1383−1391.
(32) Lemieux, R. U.; Hendriks, K. B.; Stick, R. V.; James, K. *Can. J. Chem.* **1955**, *33*, 134.
(33) Crich, D.; Chandrasekera, N. S. *Angew. Chem., Int. Ed. Engl.* **2004**, *43*, 5386−5389.
(34) Melander, L. C. S.; Saunders, W. H. Wiley-Interscience: New York 1980.
(35) Singleton, D. A.; Thomas, A. A. *J. Am. Chem. Soc.* **1995**, *117*, 9357−9358.

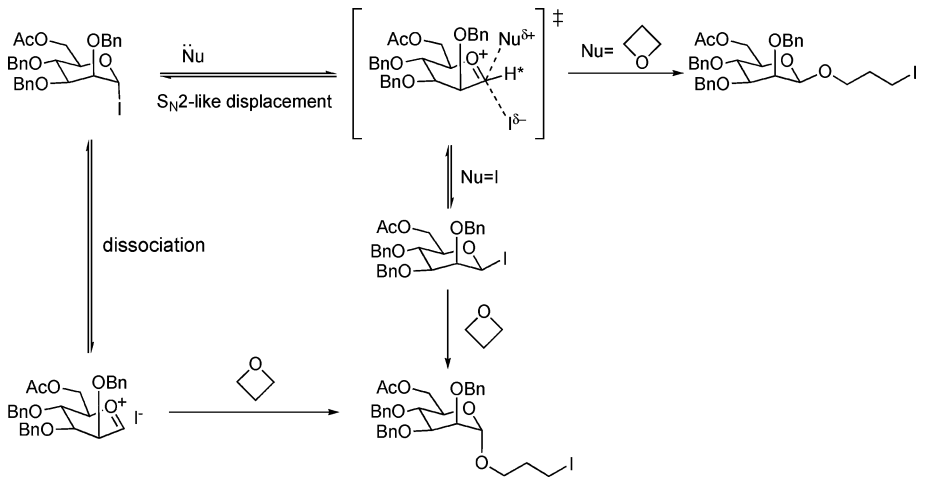

FIGURE 1. Proposed mechanisms for the mannosylation reaction of TMO.

SCHEME 4. Synthesis of 6-*O*-Deuterated Acetyl Analogue as Internal Standard

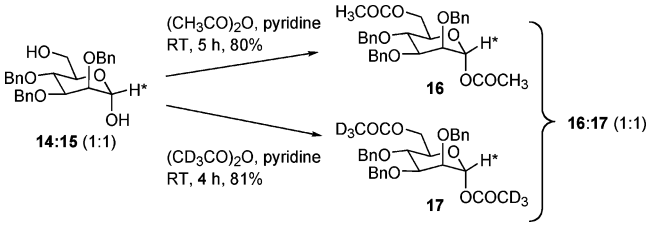

14 possessing >95% deuterium at the anomeric center is outlined in Scheme 3. Selective deacetylation of 1,6-di-*O*-acetyl-2,3,4-tri-*O*-benzyl-α-D-mannopyranosemannoside **10**[36] at the anomeric center using hydrazine acetate[37] in DMF yielded compound **11**, which was oxidized in 82% yield to the corresponding lactone **12** using tetrapropylammonium perruthenate and *N*-methyl-*N*-morpholine oxide.[38] Treatment of **12** with $NaBD_4$ afforded **13** in 80% yield,[39] which was then deacetylated with sodium methoxide in methanol to yield diol **14** (in 45% overall yield). For our kinetic studies, we required a 50/50 mixture of material with and without a deuterium label at the anomeric carbon (vide infra), so the 1-deutero diol (**14**) was then mixed in an equal quantity with unlabeled **15** to give a mixture (**14**:**15** 1:1) enriched with ∼50% deuterium at the anomeric carbon, H* **(**Scheme 4).

Separate portions of mixture **14**:**15** (1:1) were acetylated with acetic anhydride and deuterated acetic anhydride to yield mannosyl acetates **16** and **17**, respectively (Scheme 4). Combining acetate**s 16** and **17** in equimolar amounts afforded a mixture of **16**:**17** (1:1) with ∼50% enrichment in deuterium at C1 (H*) and, as internal standard to measure isotopic changes at the anomeric center in the product, ∼50% enrichment in deuterium at the C6 acetate, Ac* (Scheme 4).[33]

In the KIE experiments, mannosyl acetates **16**:**17** (1:1) and 50 mol % of benzaldehyde, an internal standard to measure the percentage conversion of the product, were first dissolved in C_6D_6 and ^{1}H NMR spectra were recorded; integration of the

SCHEME 5. Mannosylation Reaction

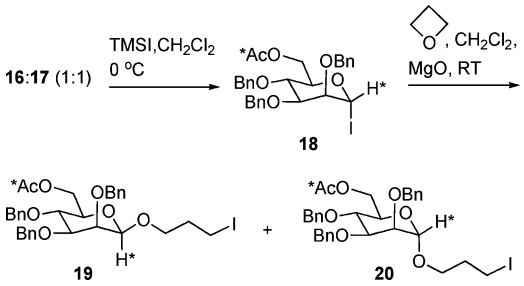

acetate peak and the anomeric hydrogens were measured against the signal of benzaldehyde (see the Experimental Section).[40] Mannosyl acetates **16**:**17** (1:1) were dissolved in CH_2Cl_2 (0.17 M), and trimethylsilyl iodide (1.1 equiv) was then added at 0 °C to produce iodides **18** quantitatively **(**Scheme 5). Next, MgO (2 equiv; added to deactivate the TMSOAc byproduct), followed by trimethylene oxide (1.5 equiv) were added to the reaction mixture at the same temperature, and then the reaction was allowed to proceed at room temperature for a particular amount of time; experiments were performed for 4, 8, and 12 h.

After aqueous workup, ^{1}H NMR spectra of the reaction mixture, containing 50 mol % of benzaldehyde, showed β-mannosides **19** as the major products and the α-anomers **20** as the minor products. The yield of the α- and β-mannosides was obtained from ^{1}H NMR integration of the C6 acetate signals against the aldehydic signal of benzaldehyde.

After HPLC separation, the ^{1}H NMR spectra of the β-mannosides were recorded with careful integration of the C6 acetates and the anomeric protons. The α-DKIE for the β-mannosides was then determined using eq 1[33]where F is the fractional

$$\mathrm{KIE} = \ln(1 - F)/\ln[1 - (FR/R_0)] \qquad (1)$$

conversion of the iodides **18** (yield of **19**), R and R_0 are the ratios of the acetates to the anomeric resonances in the products **19** and the starting acetates **16** + **17**, respectively, corresponding to the D/H ratios in **19** and **16** + **17**.

These experiments resulted in α-DKIEs of 1.16 ± 0.02, suggesting that the rate-determining transition-state structure for

(36) Tennant-Eyles, R. J.; Davis, B. G.; Fairbanks, A. J. *Tetrahedron Asymmetry* **2000**, *1*, 231−243.
(37) Murakata, C.; Ogawa, T. *Carbohydr. Res.* **1992**, *235*, 95−114.
(38) Benhaddou, R.; Czernecki, S.; Ville, G.; Zegar, A. *Carbohydr. Res.* **1994**, *260*, 243−250.
(39) Baker, D. C.; Defaye, J.; Horton, D. *J. Org. Chem.* **1976**, *41*, 3834−3840.
(40) It was taken into consideration that a ratio of 1:3 (PhCHO/Ac) from NMR integration resembles a ratio of 1:1 (PhCHO/mannosyl acetates **16:17**).

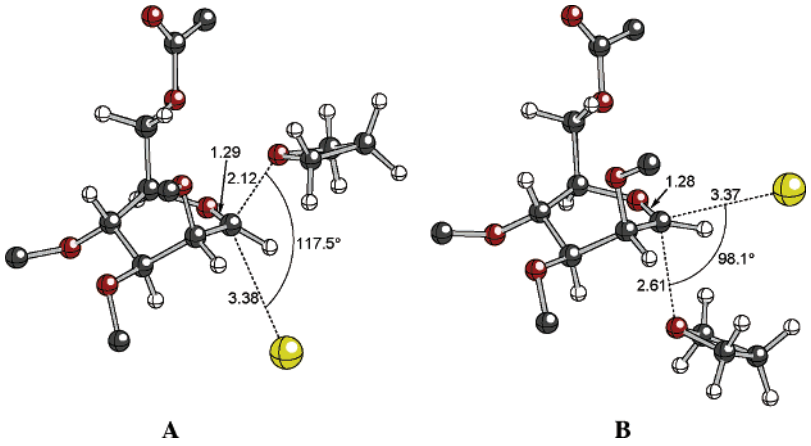

FIGURE 2. Computed geometries (B3LYP/6-31+G(d,p):LANL2DZ; selected distances in Å) of transition structures for trimethylene oxide attack on α- and *β*-mannosyl iodide models. For clarity, hydrogen atoms on methyl and acetyl groups are not shown.

this reaction has significant oxacarbenium ion character.[33] α-DKIEs for the α-anomers **20** were determined using the same methodology. In these cases, values of 1.19 ± 0.04 were obtained, also suggesting a transition-state structure with oxacarbenium ion character. As noted above, such values are consistent with both S_N1 and S_N2 processes (providing the S_N2 processes involve loose transition structures). Given the error bars on our α-DKIE values, we cannot say with certainty whether the rate-determining transition structures for formation of the α- and *β*-mannosides differ significantly in the degree to which their anomeric centers are rehybridized.

To explore these issues further, we carried out quantum chemical calculations (at the B3LYP/6-31+G(d,p):LANL2DZ level; see the Computational Methods for details) on the transition-state structures for formation of α- and *β*-mannosyl oxetanium ions. Figure 2 shows calculated transition-state structures for the direct displacement of iodide by trimethylene oxide to produce the two anomeric mannosides. In these calculations, a simplified model of the experimental system was used in which benzyl groups were replaced by methyl groups. The calculated transition structures both exhibit loose S_N2-like geometries.[41] With an O−C−I bond angle almost 20° greater than that for **B**, one might argue that **A** is more S_N2-like, but this structural variation is likely related to the nature of the gas-phase calculations used here, which should overestimate electrostatic effects; as the negatively charged iodide departs, electrostatic attraction brings it near to the somewhat positively charged proton at the anomeric center. Note that although the C−I distances are similar in both transition structures, the forming C−O bond is nearly 0.5 Å longer in **B** (axial-like attack at the anomeric carbon) than in **A** (equatorial-like attack at the anomeric carbon). In both transition structures, the C−O bond of the mannose ring is shortened, corresponding to the development of oxacarbenium (oxonium) ion character. The α-DKIEs calculated based on these transition structures (see the Methods section for details) were 1.15 for **A** and 1.26 for **B**. These values match reasonably well with experimental values, given the nature of the model systems used. Taken together, the experimentally observed and theoretically computed α-DKIEs imply that both reactions involve loose transition structures with considerable rehybridization at the anomeric center, both residing in the border regions between traditional S_N2 and S_N1 transition state structures. The calculations do suggest, though, that the transition-state structure for formation of the α C−O bond is looser than that for formation of the *β* C−O bond.

In order to investigate the possibility that the anomeric iodide may be imposing an unusual conformational constraint on the sugar ring, glycosylation reactions of conformationally locked iodides were undertaken. Cyclic restraints[42] have been used previously to facilitate the stereoselective synthesis of *β*-mannosides.[43,44] For example, the trans-fused protecting group in structures such as **21** severely decreases the flexibility of the attached sugar ring and thereby discourages formation of half-chair transition-state structures.[45,46]

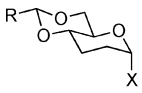

21

For comparison purposes, mannosyl acetates **23** were prepared in 93% yield from mannopyranose **22**, Scheme 6.[47,48] Treatment of **23** with TMSI in dichloromethane resulted in formation of iodide **24**, which was then coupled to TMO. The reaction was sluggish, requiring 2 days for completion; however, only the *β*-product (**25**) was obtained; no evidence was found for α-mannoside formation. The significant difference in reactivity and selectivity between **24** and **1** indicates differences in the transition states.

We also modeled the **24** to **25** transformation computationally. Our model system included a 4,6-*O*-methylene bridge rather than the 4,6-*O*-benzylidine. The α- and *β*-transition structures

(41) This may be an artifact of the gas phase nature of the calculations. The following paper nicely describes many of the issues associated with locating transition state structures for heterolytic dissociation reactions: Schreiner, P. R.; Schleyer, P. v. R.; Schaefer, H. F., III. *J. Org. Chem.* **1997**, *62*, 4216−4228. In addition, the work of Beauchamp and co-workers provides relevant experimental data on the feasibility of gas phase ionization processes; see, for example: Berman, D. W.; Anicich, V.; Beauchamp, J. L. *J. Am. Chem. Soc.* **1979**, *101*, 1239−1248.

(42) Fraser-Reid, B.; Wu, Z.; Andrews, C. W.; Skowronski, E.; Bowen, J. P. *J. Am. Chem. Soc.* **1991**, *113*, 1434−1435.

(43) Crich, D.; Sun, S. *Tetrahedron* **1998**, *54*, 8321−8348.

(44) Crich, D.; Smith, M. *J. Am. Chem. Soc.* **2002**, *124*, 8867−8869.

(45) Jensen, H. H.; Nordstrom, L. U.; Bols, M. *J. Am. Chem. Soc.* **2004**, *126*, 9205−9213.

(46) Nukada, T.; Berces, A.; Whitfield, D. M. *Carbohydr. Res.* **2002**, *337*, 765−774.

(47) Wang, W.; Kong, F. *Carbohydr. Res.* **1999**, *315*, 128−136.

(48) Codee, J. D. C.; Hossain, L. H.; Seeberger, P. H. *Org. Lett.* **2005**, *7*, 3251−3254.

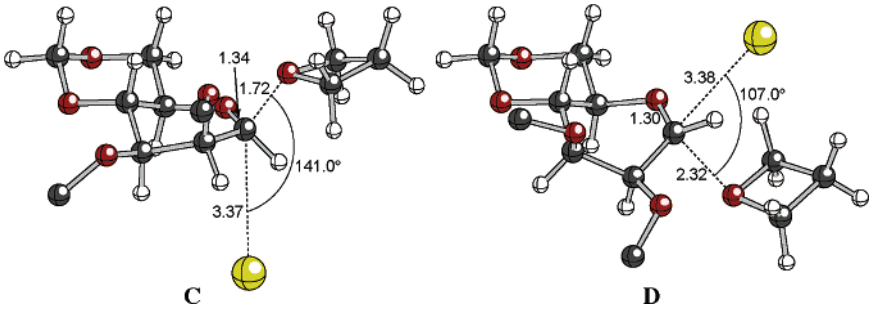

FIGURE 3. Computed geometries (B3LYP/6-31+G(d,p):LANL2DZ; selected distances in Å) of transition structures for TMO attack on methylene-bridged α- and β-mannosyl iodide models. For clarity, hydrogen atoms on methyl and acetyl groups are not shown.

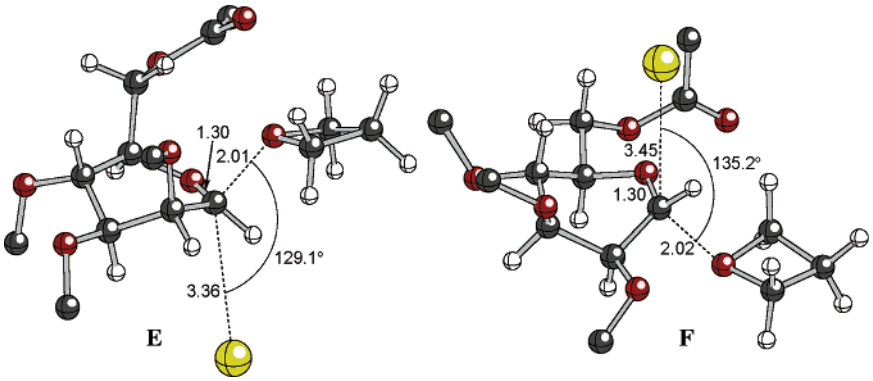

FIGURE 4. Computed geometries (B3LYP/6-31+G(d,p):LANL2DZ; selected distances in Å) of transition structures for trimethylene oxide attack on α- and β-mannosyl iodide models. For clarity, hydrogen atoms on methyl and acetyl groups are not shown.

SCHEME 6. Generation and Reaction of 4,6-*O*-Benzylidine-D-mannosyl Iodide with TMO

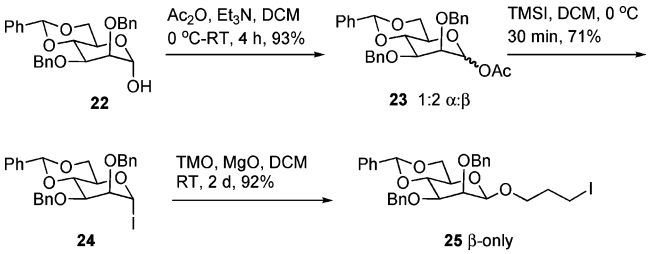

for this substrate are shown in Figure 3. These transition-state structures can be thought of as ring-flipped analogues of the corresponding transition structures in Figure 2. The geometries around the anomeric carbon are notably different than those in Figure 2; for example, the computed C−O distances of 1.72 and 2.32 Å for **C** and **D**, respectively, are significantly shorter than their nonbridged counterparts. Nonetheless, the C−I distance only differs by 0.01 Å across all four transition structures, suggesting that in all four cases the C−I bond has been effectively broken by the time the transition structure is reached (i.e., although all four transition-state structures correspond to concerted displacements of iodide by TMO, the bond-breaking and -forming events happen asynchronously). In addition, note that the conformations of **C** and **D** are considerably different from each other, since the C−H group at the anomeric center must orient itself differently in each case so as to allow for C−O bond formation without excessive steric problems.

Having located transition-state structures resembling ring-flipped analogues of those in Figure 2, it was of particular interest to see if ring-flipped versions of **A** and **B** exist without an acetal bridge. After a series of constrained calculations starting with the geometries of **C** and **D** (see the Methods section for details), the fully optimized transition structures shown in Figure 4 were located. While structure **F**, leading to the α-product, has a ring conformation similar to that of structure **D**, structure **E**, despite all attempts, always fell back to a structure with the same conformation of the sugar ring found for **A** (compare with Figure 2).[49]

While experimental KIE measurements for the bridged system were not explored, theoretical KIE values were calculated on the basis of transition structures **C** and **D** (as well as **E** and **F**), and these allow us to relate geometric differences to changes in KIE values for a variety of similar systems. Calculated KIE values for structures **A**, **B**, **C**, **D**, **E**, and **F** are 1.15, 1.26, 1.01, 1.31, 1.09, and 1.08, respectively. There is a rough correlation between the C−O distances in these transition structures and their calculated KIE values—in general, larger KIE values are associated with longer C−O (partial) bonds (Figure 5), although the correlation is not perfect (since the KIEs depend on many factors in addition to the degree of C−O bonding).

In general, pairs of related transition structures (**A** and **B**; **C** and **D**) were close to each other in energy (i.e., within a few kcal/mol of each other), and the member of each pair with a larger C−O distance was lower in energy (see the Supporting

(49) It is important to highlight that although the same ring conformation is present in structures **A** and **E**, the methoxy and acetate groups adorning these sugars assume different conformations. There is no doubt that these two minima represent a narrow sampling of possible conformations for these groups, but computational resources and the nature of the model system itself, specifically the substitution of methyl groups for benzyl groups, made an exhaustive search of this conformational space not only impractical, but also unwarranted. Note also that both of the transition structures in Figure 4 are higher energy conformers than their analogs in Figure 2: **E** is 2.9 kcal/mol higher than **A**, and **F** is 14.2 kcal/mol higher than **B**.

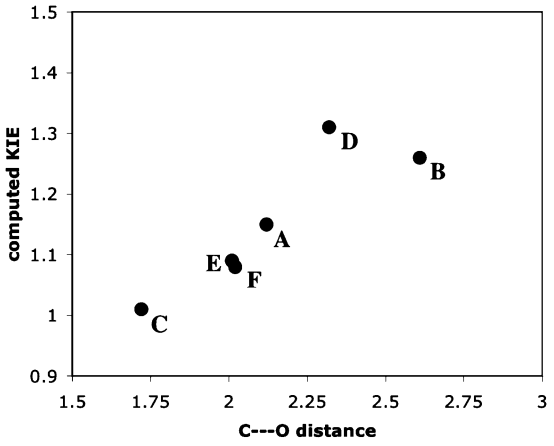

FIGURE 5. Correlation between computed KIEs and C−O distances.

Information for details). These relative energies do not correspond to the experimental distributions of products, but this is likely a result of the simplified model systems used and the fact that these energies are for gas-phase structures. We have, to this point, had impenetrable difficulties with solvation calculations on these systems. Nonetheless, correspondence between calculated and experimental isotope effects is still a valid measure of the plausibility of the *geometry* of a transition-state structure.

Conclusion

α-DKIEs for the mannosylation reaction of mannosyl iodide with trimethylene oxide were determined experimentally to be ∼1.16 and ∼1.19 for the *β*- and α-mannosides, respectively. These values suggest that both cases have rate-determining transition structures with significant oxacarbenium ion character. Acyl participation at the anomeric center does not take place in these reactions, and the anomeric iodide present in these systems does not bias the ring conformations as bridging acetal protecting groups do. Quantum chemical calculations revealed details of the transition structure geometries for these reactions, showing that the observed KIEs are consistent with very loose S_N2-like processes.

Experimental

6-*O*-*tert*-Butyldimethylsilyl-α-methyl-D-mannopyranoside (4). To a stirred solution of α-methyl-D-mannopyranoside **3** (1.5 g, 7.7 mmol), triethylamine (3.76 g, 27 mmol), and DMAP (47 mg, 0.39 mmol) in DMF (12 mL) at 0 °C was added TBDMSCl (1.28 g, 8.5 mmol). The reaction was then allowed to proceed at room temperature for 12 h. Upon reaction completion, the mixture was poured over ice−water (10 mL) and extracted with dichloromethane (50 mL), and the organic mixture was washed with ammonium chloride and water (10 mL, each). The organic extract was then dried over Na_2SO_4 and stripped of solvent in vacuo, and the concentrated residue was purified by column chromatography, $R_f = 0.25$ (hexanes/ethyl acetate 1:4), to afford the title compound (82%) as a white solid: mp 102.1−103.0; $[\alpha]^{23}_D$ +57 (*c* 0.3 in $CHCl_3$); IR *ν* 3386, 2938, 2857, 1100, 1049, 839; ^{1}H NMR (600 MHz, C_6D_6) *δ* 0.21 (s, 6 H), 1.04 (s, 9 H), 3.25 (s, 3 H), 3.82−3.86 (m, 1 H), 4.02−4.07 (m, 2 H), 4.11−4.14 (m, 1 H), 4.20 (d, 1 H, $J = 2.4$ Hz), 4.22 (d, 1 H, $J = 3.0$ Hz), 4.56 (d, 1 H, $J = 4.8$ Hz), 4.61 (d, 1 H, $J = 3.6$ Hz), 4.84 (d, 1 H, 1.2 Hz, H-1α), 5.12 (d, 1 H, $J = 5.4$ Hz); ^{13}C NMR (150 MHz, C_6D_6) *δ* −5.2, −5.2, 18.5, 26.1, 54.4, 64.2, 68.9, 71.1, 72.5, 73.2, 101.3; HR-EI-MS *m*/*z* $[M]^+$ calcd for $C_{13}H_{28}O_6Si_1$ 308.1650, found 308.1637.

6-*O*-*tert*-Butyldimethylsilyl-2,3,4-tri-*O*-benzyl-α-methyl-D-mannopyranoside (5). To a stirred solution of 6-*O*-*tert*-butyldimethylsilyl-α-methyl-D-mannopyranoside **4** (1.9 g, 6.15 mmol), benzyl bromide (2.94 g, 24.6 mmol), and tetrabutylammonium iodide (113 mg, 0.31 mmol) in DMF (23 mL) at 0 °C was added NaH (0.81 g, 33.83 mmol). The reaction was then allowed to continue at rt for 24 h. Upon reaction completion, the mixture was quenched with methanol (5 mL) and diluted with ethyl acetate (30 mL). The organic mixture was washed with water (10 mL), and the aqueous extraction was washed with ether (2 × 30 mL). The organic extract was combined and dried over Na_2SO_4 to afford the title compound (67%) as a colorless syrup, $R_f = 0.77$ (toluene/ethyl acetate 85:15). The concentrated residue was then purified by column chromatography (15% ethyl acetate in hexanes): $[\alpha]^{23}_D$ +21.6 (*c* 1.9 in $CHCl_3$); IR *ν* 2929, 1102, 1059; ^{1}H NMR (600 MHz, C_6D_6) *δ* 0.07 (s, 3 H), 0.10 (s, 3 H), 0.97 (s, 9 H), 3.09 (s, 3 H), 3.71 (dd, 1 H, $J = 3.6$ and 13.2 Hz), 3.74 (t, 1 H, $J = 2.4$ Hz), 3.85 (dd, 1 H, $J = 1.4$ and 11.0 Hz), 3.91 (dd, 1 H, $J = 4.8$ and 11.4 Hz), 4.02 (dd, 1 H, $J = 3.0$ and 9.6 Hz), 4.18 (t, 1 H, $J = 9.6$ Hz), 4.40−4.49 (m, 3 H), 4.58 (d, 1 H, $J = 12$ Hz), 4.66 (d, 1 H, $J = 10.8$ Hz), 4.68 (d, 1 H, $J = 1.8$ Hz), 4.99 (d, 1 H, $J = 11.4$ Hz), 7.03−7.33 (m, 15 H, ArH); ^{13}C NMR (150 MHz, C_6D_6) *δ* −4.8, −4.9, 18.7, 26.3, 54.5, 63.3, 72.4, 73.2, 73.9, 75.3, 75.4, 76.0, 81.1, 99.6, 127.7, 127.8, 127.83, 128.0, 128.02, 128.2, 128.3, 128.5, 128.6, 128.63, 128.7, 139.4, 139.5, 139.9; HR-EI-MS *m*/*z* $[M]^+$ calcd for $C_{34}H_{46}O_6Si_1$ 578.3058, found 578.3055.

2,3,4-Tri-*O*-benzyl-α-methyl-D-mannopyranoside (6). To a stirred solution of 6-*O*-*tert*-butyldimethylsilyl-2,3,4-tri-*O*-benzyl-α-methyl-D-mannopyranoside **5** (1.7 g, 2.9 mmol) and MS, 4 Å (40 mg) in THF was added tetrabutylammonium fluoride (8.8 mL, 1 M in THF) at 0 °C. The reaction was then allowed to proceed at room temperature for 6 h. Upon reaction completion, the mixture was concentrated in vacuo and diluted with ethyl acetate (50 mL), and the organic mixture was washed with sodium bicarbonate (10 mL) and water (10 mL). The aqueous extract was washed with dichloromethane, and the combined organic extracts were dried over Na_2SO_4. The concentrated residue was purified by column chromatography, $R_f = 0.57$ (hexanes/ethyl acetate 1:1) to afford the title compound (67%) as a colorless syrup: $[\alpha]^{23}_D$ +42.4 (*c* 0.45 in $CHCl_3$); IR *ν* 3467, 2906, 1454, 1109, 1071; ^{1}H NMR (150 MHz, $CDCl_3$) *δ* 2.40 (brs, 1 H) 3.34 (s, 3 H), 3.67 (m, 1 H), 3.82−3.92 (m, 3 H), 3.97 (dd, 1 H, $J = 3.0$ and 9.0 Hz), 4.04 (t, 1 H, $J = 9.6$ Hz), 4.68 (d, 1 H, $J = 2.4$ Hz), 4.71−5.01 (m, 6 H, CH_2Ph), 7.25−7.42 (m, 15 H, ArH); ^{13}C NMR (150 MHz, $CDCl_3$) *δ* 54.7, 62.3, 72.2, 72.22, 72.9, 74.7, 74.8, 75.2, 80.2, 99.3, 127.6, 127.7, 127.73, 127.9, 128.0, 128.4, 128.41, 138.2, 138.50. HR-EI-MS *m*/*z* $[M]^+$ calcd for $C_{28}H_{32}O_6$ 464.2193, found 464.2206.

6-*O*-(4-Nitrobenzyl)-2,3,4-tri-*O*-benzyl-α-methyl-D-mannopyranoside (7). To a stirred solution of 2,3,4-tri-*O*-benzyl-α-methyl-D-mannopyranoside **6** (170 mg, 0.4 mmol) and chlorotrimethylsilane (0.47 mL, 3.7 mmol) in CH_2Cl_2 (2.0 mL) were added 4-nitrobenzaldehyde (55 mg, 0.4 mmol) and triethylsilane (0.12 mL, 0.7 mmol). The reaction was stirred at rt for 2 d. Upon reaction completion, the reaction mixture was concentrated under vacuum and the organic residue was subjected to column chromatography, $R_f = 0.27$ (hexane/ethyl acetate 75:25), to afford the benzylated compound (76%) as a colorless syrup: $[\alpha]^{23}_D$ +37.1 (*c* 1.0 in $CHCl_3$); IR *ν* 2900, 1520, 1106; ^{1}H NMR (600 MHz, $CDCl_3$) *δ* 3.35 (s, 3 H), 3.76−3.79 (m, 2 H), 3.83−3.86 (m, 2 H), 3.94 (dd, 1 H, $J = 3.0$ and 9.6 Hz), 4.03 (t, 1 H, $J = 9.6$ Hz), 4.57−4.64 (m, 4 H), 4.71−4.80 (m, 4 H), 4.96 (d, 1 H, $J = 11.4$ Hz), 7.22−7.40 (m, 15 H, ArH), 7.47 (d, 2 H, $J = 8.4$ Hz), 8.12 (d, 2 H, $J = 8.4$ Hz); ^{13}C NMR (150 MHz, $CDCl_3$) *δ* 55.1, 70.2, 71.9, 72.1, 72.3, 73.0, 74.8, 74.9, 75.3, 80.4, 99.3, 123.8, 127.8, 127.9, 127.93, 127.94, 128.0, 128.03, 128.1, 128.6, 128.63, 128.64, 138.5, 138.7, 138.72, 146.4, 147.4. HR-EI-MS *m*/*z* $[M]^+$ calcd for $C_{35}H_{37}O_8N_1$ 599.2514, found 599.2524.

6-*O*-(4-Nitrobenzyl)-2,3,4-tri-*O*-benzyl-1-*O*-acetyl-α-D-mannopyranoside (8). To a stirred solution of 6-*O*-(4-nitrobenzyl)-

2,3,4-tri-*O*-benzyl-α-methyl-D-mannopyranoside **7** (250 mg, 0.4 mmol) and acetic anhydride (0.19 mL, 1.9 mmol) in acetic acid (0.83 mL) was added sulfuric acid (37 μL) dropwise at 0 °C for 30−60 min. Upon completion, the reaction was poured over ice−water (10 mL) and stirred for 20 min. The reaction mixture was then extracted with chloroform (50 mL) and washed with sodium bicarbonate (10 mL) and then water (10 mL). The aqueous phase was washed with chloroform (50 mL), the combined organic phase was dried over sodium sulfate and concentrated in vacuo, and the concentrated residue was then purified using column chromatography, $R_f = 0.24$ (hexane/ethyl acetate 75:25), to afford mannosyl acetate **8** (84%) as a colorless syrup: $[\alpha]^{23}_D$ +31.6 (*c* 2.85 in $CHCl_3$); IR *ν* 2891, 1748, 1519, 1344; ^{1}H NMR (600 MHz, $CDCl_3$) *δ* 2.04 (s, 3 H), 3.74 (d, 1 H, $J = 9.6$ Hz), 3.77 (t, 1 H, $J = 2.4$ Hz), 3.84 (m, 2 H), 3.90 (dd, 1 H, $J = 3.0$ and 9.6 Hz), 4.12 (t, 1 H, $J = 9.3$ Hz), 4.58−4.96 (m, 8 H, CH_2Ph), 6.22 (d, 1 H, $J = 2.4$ Hz), 7.23−7.40 (m, 15 H, ArH), 7.44 (d, 2 H, $J = 7.8$ Hz), 8.10 (d, 2 H, $J = 9.0$ Hz); ^{13}C NMR (150 MHz, $CDCl_3$) *δ* 21.1, 69.6, 72.3, 72.33, 72.8, 73.6, 74.1, 74.5, 75.4, 79.3, 91.8, 123.6, 127.8, 127.9, 127.92, 127.94, 128.0, 128.03, 128.1, 128.5, 128.54, 137.8, 138.1, 138.3, 146.1, 147.3, 169.1; HR-EI-MS *m*/*z* $[M]^+$ calcd for $C_{36}H_{37}O_9N_1$ 627.2463, found 627.2453.

1-*O*-(3-Iodopropyl)-6-*O*-(4-nitrobenzyl)-2,3,4-tri-*O*-benzyl-α-D-mannopyranoside (9). To a stirred solution of 6-*O*-(4-nitrobenzyl)-2,3,4-tri-*O*-benzyl-1-*O*-acetyl-α-D-mannopyranoside **8** (87 mg, 0.14 mmol) in dichloromethane (0.8 mL, 0.2 mmol) was added trimethylsilyl iodide (21 μL, 0.2 mmol) at 0 °C for 1 h to show complete formation of the iodide. MgO (11 mg, 0.28 mmol) followed by trimethylene oxide (14 μL, 0.21 mmol) was added to the reaction mixture at the same temperature, and then the reaction was allowed to proceed at room temperature for 6 h. Upon completion, the reaction was diluted with ethyl acetate (30 mL), and the organic mixture was washed with sodium thiosulfate, brine, and water (5 mL, each). The aqueous phase was washed with dichloromethane (30 mL), and the combined organic phase was dried over sodium sulfate and concentrated in vacuo to afford mannoside **9** (86% of 1:4 α/*β*) as a colorless syrup. Purification of the crude residue and separation of the anomers was achieved successfully using column chromatography (15% ethyl acetate in hexane). For the major product (*β*-anomer), $R_f = 0.63$ (toluene/ethyl acetate 85:15); ^{1}H NMR (600 MHz, C_6D_6) *δ* 1.68 (m, 2 H), 2.85−2.92 (m, 2 H), 3.21 (m, 1 H), 3.27−3.30 (m, 2 H), 3.59 (d, 1 H, $J = 1.2$ and 11.4 Hz), 3.67−3.72 (m, 3 H) 3.95 (s, 1 H), 4.06 (m, 1 H), 4.17−4.98 (m, 8 H, CH_2Ph), 6.94−7.80 (m, 19 H, ArH); ^{13}C NMR (150 MHz, C_6D_6) *δ* 3.1, 33.2, 68.8, 70.1, 71.3, 72.1, 74.5, 74.9, 75.0, 75.1, 76.2, 82.4, 101.9, 123.4, 127.6, 127.64, 127.7, 127.72, 127.74, 127.9, 128.1, 128.2, 128.4, 128.43, 128.6, 138.8, 139.2, 139.4, 146.0, 147.5; HR-EI-MS *m*/*z* $[M]^+$ calcd for $C_{37}H_{40}O_8I_1N_1$ 753.1793, found 753.1773. For the minor product (α-anomer), $R_f = 0.62$ (toluene/ethyl acetate 85:15); ^{1}H NMR (600 MHz, C_6D_6) *δ* 1.56 (m, 2 H), 2.75 (t, 2 H, $J = 6.6$ Hz), 3.09 (m, 1 H), 3.55 (m, 1 H), 3.61 (dd, 1 H, $J = 1.8$ and 6.3 Hz), 3.73−3.77 (m, 2 H), 3.89 (dd, 1 H, $J = 3.6$ and 9.6 Hz), 3.99 (dd, 1 H, $J = 3.0$ and 9.0 Hz), 4.14 (d, 1 H, $J = 13.2$ Hz), 4.23 (t, 1 H, $J = 9.6$ Hz), 4.29 (d, 1 H, $J = 13.2$ Hz), 4.44 (d, 1 H, $J = 3.6$ Hz), 4.47 (d, 1 H, $J = 12.0$ Hz), 4.55 (d, 1 H, $J = 11.4$ Hz), 4.62 (d, 1 H, $J = 12.0$ Hz), 4.81 (d, 1 H, $J = 1.2$ Hz), 5.00 (d, 1 H, $J = 11.4$ Hz), 6.93−7.79 (m, 19 H, ArH); ^{13}C NMR (150 MHz, C_6D_6) *δ* 2.5, 33.0, 67.0, 70.2, 72.1, 72.2, 73.0, 73.2, 75.2, 75.6, 80.6, 98.6, 123.4, 127.5, 127.6, 127.7, 127.8, 127.9, 128.0, 128.1, 128.2, 128.3, 128.4, 128.5, 128.52, 183.8, 138.9, 139.2, 146.0, 147.5. HR-EI-MS *m*/*z* $[M]^+$ calcd for $C_{37}H_{40}O_8I_1N_1$ 753.1793, found 753.1762.

6-*O*-Acetyl-2,3,4-tri-*O*-benzyl-α-D-manno-1-lactone (12) A mixture of 6-*O*-acetyl-2,3,4-tri-*O*-benzyl-α-D-mannopyranose **11** (1.14 g, 2.3 mmol), tetrapropylammonium perruthenate (81 mg, 0.231 mmol), *N*-methyl-*N*-morpholine oxide (0.54 g, 4.63 mmol) and MS, 3 Å (0.57 g) in CH_2Cl_2 (19 mL) was stirred at room temperature for 2 h. Upon reaction completion, the mixture was diluted with dichloromethane (50 mL) and washed with 5% sodium sulfite in brine, brine, and copper sulfate (10 mL, each). The combined organic extract was dried over $MgSO_4$, filtered through Celite, and concentrated in vacuo, and the concentrated residue was purified by column chromatography, $R_f = 0.53$ (hexanes,ethyl acetate/ 2:1), to afford the title compound (93%, as an oil): $[\alpha]^{23}_D$ +22 (*c* 0.1 in $CHCl_3$); IR *ν* 2910, 1776, 1454, 1142, 1084; ^{1}H NMR (600 MHz, $CDCl_3$) *δ* 2.02 (s, 3 H, Ac), 3.65 (d, 1 H, $J = 7.8$ Hz), 4.08 (m, 1 H), 4.17 (dd, 1 H, $J = 6.6$ and 12.0 Hz), 4.22−4.27 (m, 3 H), 4.36−4.38 (m, 2 H), 4.60 (d, 1 H, $J = 12$ Hz), 4.67 (d, 1 H, $J = 12$ Hz), 4.88 (d, 1 H, $J = 12$ Hz), 4.08 (d, 1 H, $J = 12$ Hz), 7.15−7.41 (m, 15 H, ArH); ^{13}C NMR (150 MHz, $CDCl_3$) *δ* 20.9, 63.4, 72.0, 73.2, 73.4, 75.6, 76.4, 76.5, 76.6, 128.1, 128.2, 128.3, 128.4, 128.5, 128.6, 128.7, 128.8, 136.6, 137.2, 137.7, 169.1, 170.8. HR-EI-MS *m*/*z* $[M]^+$ calcd for $C_{29}H_{30}O_7$ 490.1986, found 490.1995.

1-Deutero-6-*O*-acetyl-2,3,4-tri-*O*-benzyl-D-mannopyranose (13). To a mixture of 6-*O*-acetyl-2,3,4-tri-*O*-benzyl-α-D-manno-1-lactone **12** (684 mg, 1.4 mmol) and sodium borodeuteride (88 mg, 2.1 mmol) in methanol (50 mL, 0.028 M) was added water (3.5 mL) at 0 °C. After 3 min, the reaction reached completion, and the mixture was neutralized with CO_2 gas bubbled in the solution. The reaction mixture was azeotroped with methanol (4 × 15 mL) to remove boric acid as its methyl ester followed by azeotroping with toluene (3 × 15 mL). The mixture was concentrated and then diluted in chloroform (30 mL) and washed with water (2 × 5 mL). The combined organic extract was dried over Na_2SO_4 and concentrated in vacuo, and the concentrated residue was purified by column chromatography, $R_f = 0.54$ (hexanes/ethyl acetate/ 1:1), to afford oil **13** (80%, 1:5 *β*:α). For the major product (α-anomer): ^{1}H NMR (600 MHz, $CDCl_3$) *δ* 2.05 (s, 3 H, Ac), 3.84 (d, 1 H, $J = 4.2$ Hz), 3.97 (t, 1 H, $J = 9.6$ Hz), 4.02−4.09 (m, 2 H), 4.30 (dd, 1 H, $J = 5.4$ and 11.4 Hz), 4.41 (dd, 1 H, $J = 1.8$ and 12.0 Hz), 4.64−4.67 (m, 3 H), 4.71 (d, 1 H, $J = 12.0$ Hz), 4.77 (d, 1 H, $J = 12.6$ Hz), 4.99 (d, 1 H, $J = 10.8$ Hz), 7.31−7.42 (m, 15 H, ArH); ^{13}C NMR (150 MHz, $CDCl_3$) *δ* 20.9, 63.8, 70.0, 72.1, 72.6, 74.6, 74.8, 75.2, 79.6, 92.2 (t, $^1J_{CD} = 79.03$ Hz), 127.72, 127.73, 127.74, 127.81, 127.83, 128.0, 128.1, 128.2, 128.22, 128.3, 128.4, 128.42, 128.5, 128.53, 128.6, 128.62, 129.1, 137.8, 138.0, 138.2, 138.3, 138.33, 171.3. Some selected values for the minor product (*β*-anomer): ^{1}H NMR (600 MHz, $CDCl_3$) *δ* 3.56 (m, 1 H), 3.67 (dd, 1 H, $J = 2.7$ and 9.3 Hz), 3.90 (m, 1 H), 5.13 (d, 1 H, $J = 11.4$ Hz); ^{13}C NMR (150 MHz, $CDCl_3$) *δ* 63.6, 72.7, 73.3, 74.2, 75.8, 83.0, 171.1. HR-EI-MS *m*/*z* $[M]^+$ calcd for $C_{29}H_{31}{}^2H_1O_7$ 493.2205, found 493.2201.

1-Deutero-2,3,4-tri-*O*-benzyl-D-mannopyranose (14). To a stirred solution of 1-deutero-6-*O*-acetyl-2,3,4-tri-*O*-benzyl-α-D-mannopyranose **13** (440 mg, 0.9 mmol) in methanol (6 mL, 0.15 M) was added sodium methoxide, 30% in methanol (150 μL, 2.7 mmol) at 0−10 °C for 30 min. Upon reaction completion, the mixture was neutralized with acidic resin, DOWEX 50wx 2-200, the neutral mixture was filtered out, and the filtrate was concentrated and then filtered through a short plug of silica gel, $R_f = 0.20$ (hexanes/ethyl acetate/ 1:1), to afford syrup **14** (93%, 1:6 *β*/α). For the major product (α-anomer): ^{1}H NMR (400 MHz, C_6D_6) *δ* 3.55 (m, 1 H), 3.80 (d, 2 H, $J = 2.4$ Hz), 3.97 (m, 1 H), 4.04 (t, 1 H, $J = 9.6$ Hz), 4.15 (dd, 1 H, $J = 2.8$ and 9.2 Hz), 4.19 (m, 1 H), 4.35−4.91 (m, 6 H, CH_2Ph), 7.01−7.35 (m, 15 H, ArH); ^{13}C NMR (100 MHz, C_6D_6) *δ* 62.9, 72.3, 73.0, 73.3, 75.3, 76.0, 76.3, 80.5, 92.8 (m, C−D), 127.6, 127.63, 127.7, 127.72, 127.74, 127.9, 128.0, 128.03, 128.1, 128.2, 128.3, 128.4, 128.43, 128.5, 128.6, 128.62, 138.7, 138.72, 138.9, 139.0, 139.1. Some selected values for the minor product (*β*-anomer): ^{1}H NMR (400 MHz, C_6D_6) 3.19−3.22 (m, 1 H), 3.24 (dd, 1 H, $J = 2.8$ and 2.0), 3.41 (t, 1 H, $J = 6.0$ Hz), 3.86 (d, 1 H, $J = 2.8$), 3.89 (m, 1 H); ^{13}C NMR (100 MHz, C_6D_6) *δ* 62.2, 72.5, 75.0, 75.2, 76.4, 76.7, 83.2. 92.8; HR-EI-MS *m*/*z* $[M]^+$ calcd for $C_{27}H_{29}{}^2H_1O_6$ 451.2100, found 451.2095.

2,3,4-Tri-*O*-benzyl-D-mannopyranose (15). To a stirred solution of 1,6-di-*O*-acetyl-2,3,4-tri-*O*-benzyl-α-D-mannopyranoside **10**

(0.74 g, 1.4 mmol) in methanol/THF, 3:1 (12 mL) was added sodium methoxide (30% in methanol), 0.47 mL, 8.34 mmol, at 0−10 °C for 40 min. Upon reaction completion, the mixture was neutralized with acidic resin, DOWEX 50wx 2-200, the neutral mixture was filtered, and the filtrate was concentrated and then filtered through a short plug of silica gel, $R_f = 0.20$ (hexanes/ethyl acetate 1:1), to afford syrup **8** (93%, 1:8 β/α). For the major product (α-anomer): ^{1}H NMR (400 MHz, $CDCl_3$) δ 3.48 (t, 1 H, J = 6.0 Hz), 3.70 (m, 1 H), 3.81−3.90 (m, 2 H), 3.97 (bd, 1 H J = 8.8 Hz), 4.03 (dd, 1 H, J = 2.8 and 12.0 Hz), 4.63−4.98 (m, 6 H, CH_2Ph), 5.13 (bd, 1 H, J = 1.2 Hz), 7.31−7.42 (m, 15 H, ArH); ^{13}C NMR (100 MHz, $CDCl_3$) 62.5, 72.1, 72.2, 73.0, 75.2, 75.3, 75.5, 79.9, 92.6, 127.6, 127.7, 127.8, 127.83, 127.9, 128.0, 128.1, 128.2, 128.2, 128.4, 128.5, 128.53, 128.6, 138.2, 138.24, 138.4. Some selected values for the minor product (β-anomer): ^{1}H NMR (400 MHz, $CDCl_3$) 3.25 (t, 1 H, J = 6.4 Hz), 3.34−3.38 (m, 1 H), 3.42 (d, 1 H, J = 6.0 Hz), 3.61 (m, 1 H); ^{13}C NMR (100 MHz, $CDCl_3$) δ 62.0, 72.6, 74.4, 75.5, 75.8, 82.8, 94.1; HR-EI-MS m/z $[M]^+$ calcd for $C_{27}H_{30}O_6$ 450.2037, found 450.2043.

1-(50% Deutero)-1,6-di-*O*-acetyl-2,3,4-tri-*O*-benzyl-α-D-mannopyranoside (16). To a stirred solution of a 1:1 mixture of mannopyranoses **14** and **15** (100 mg, 0.22 mmol) in pyridine (1.5 mL) was added acetic anhydride (0.82 μL, 0.9 mmol) at rt for 5 h. Upon reaction completion, the mixture was diluted with ethyl acetate (25 mL), neutralized with aqueous HCl (10%), washed with water (5 mL), and dried (Na_2SO_4). The residue was purified by column chromatography, $R_f = 0.66$ (hexanes/ethyl acetate 3:2), to afford the title compound (80%) as a white solid: mp 88.3−91.6 °C; $[\alpha]^{23}_D$ +31.8 (c 0.55 in $CHCl_3$); IR ν 3031, 2902, 1743, 1231, 1094; ^{1}H NMR (400 MHz, $CDCl_3$) δ 2.06 (s, 3 H, Ac), 2.08 (s, 3H, Ac), 3.79 (t, 1 H, J = 2.8 Hz), 3.93 (m, 2 H), 4.05 (dd, 1 H, J = 9.6, 9.6 Hz), 4.37 (m, 2 H), 4.63−4.67 (m, 3 H), 4.80 (q, 2 H, J = 12.4 and 9.2 Hz), 5.00 (d, 1 H, J = 10.8 Hz), 6.24 (d, 0.5 H, J = 2.00 Hz, H-1α), 7.26−7.41 (m, 15 H, ArH); ^{13}C NMR (100 MHz, $CDCl_3$) δ 20.9, 21.0, 63.1, 72.0, 72.3, 73.0, 73.1, 73.7, 75.3, 79.0, 91.5, 127.7, 127.8, 127.82, 127.9, 128.1, 128.3, 128.4, 128.5, 137.7, 137.9, 168.8, 170.8. HR-EI-MS m/z $[M]^+$ calcd for $C_{31}H_{34}O_8$ 534.2248 and $C_{31}H_{33}{}^2H_1O_8$ 535.2311, found 534.2255 and 535.2308, respectively.

1-(50% Deutero)-1,6-di-*O*-(acetyl-*d*$_3$)-2,3,4-tri-*O*-benzyl-α-D-mannopyranoside (17). To a stirred solution of a 1:1 mixture of mannopyranoses **14** and **15** (200 mg, 0.44 mmol) in pyridine (3 mL, 0.15 M) was added deuterated acetic anhydride (0.17 mL, 1.76 mmol) at rt for 4 h. Upon reaction completion, the mixture was diluted with ethyl acetate (30 mL), neutralized with aqueous HCl (10%), washed with water (2 × 5 mL), and dried (Na_2SO_4). The residue was purified by column chromatography, $R_f = 0.66$ (hexanes:ethyl acetate 3:2), to afford the title compound (81%) as white crystals: mp 88.5−93.9; ^{1}H NMR (400 MHz, $CDCl_3$) δ 3.76 (d, 1 H, J = 2.4 Hz), 3.90 (dd, 2 H, J = 2.8, 9.2 Hz), 4.01 (m, 1 H), 4.34 (m, 2 H), 4.62 (m, 3 H), 4.76 (q, 2 H, J = 12.40 and 9.6 Hz), 4.97 (d, 1 H, J = 10.8 Hz), 6.21 (d, 0.5 H, J = 2.4 Hz, H-1α), 7.26−7.41 (m, 15 H, ArH); ^{13}C NMR (100 MHz, $CDCl_3$) δ 21.05 (m, C−D_3), 63.2, 72.1, 72.4, 72.41, 72.42, 73.1, 73.2, 73.8, 75.5, 79.1, 91.6, 127.8, 127.9, 127.9, 128.0, 128.3, 128.5, 128.54, 128.6, 137.8, 138.0, 138.02, 167.0, 171.0. HR-EI-MS m/z $[M]^+$ calcd for $C_{31}H_{28}{}^2H_6O_8$ 540.2472 and $C_{31}H_{27}{}^2H_7O_8$ 541.2688, found 540.2474 and 541.2683, respectively.

1-(50% Deutero)-1-β-*O*-(3-iodopropyl)-2,3,4-tri-*O*-benzyl-6-*O*-(acetyl-50% *d*)-D-mannopyranoside (19) and 1-(50% Deutero)-1-α-*O*-(3-iodo-propyl)-2,3,4-tri-*O*-benzyl-6-*O*-(acetyl-50% *d*)-D-mannopyranoside (20). A mixture of a 1:1 ratio of mannopyranosides **16** and **17** (86 mg, 0.16 mmol) and benzaldehyde (8.2 μL, 0.08 mmol) were dissolved in C_6D_6, and the ^{1}H NMR spectrum was recorded. Mannosyl acetates **16** + **17** were dissolved in CH_2Cl_2 (0.9 mL) at 0 °C, and TMSI (26 μL, 0.19 mmol) was added to produce iodides **18** with complete conversion. MgO (13 mg, 0.3 mmol) followed by trimethylene oxide (16 mg, 0.2 mmol) were added at 0 °C, and the mixture was then stirred at rt for 4, 8, and 12 h. The reaction mixture was diluted with CH_2Cl_2 (20 mL) and washed with satd $Na_2S_2O_3$ (2 × 5 mL) and brine (2 × 5 mL). The organic extract was dried (Na_2SO_4) and concentrated in vacuo to afford mixture of anomers **19** + **20**, $R_f = 0.57$ (toluene/ethyl acetate 85:15). Benzaldehyde (8.2 μL) was added to the reaction mixture, and the ^{1}H NMR spectrum was recorded. The crude mixture was then purified using analytical normal-phase HPLC (Si phase, isocratic elution with ethyl acetate:petroleum ether (15:85), 1 mL/min. flow, detection at 260 nm) to give complete separation of the α and the β anomers as colorless oils. For the major product (β-anomer): $[\alpha]^{23}_D$ −2.4 (c 0.5 in $CHCl_3$); IR ν 3031, 2893, 1738, 1346, 1092; ^{1}H NMR (600 MHz, C_6D_6) δ 1.63 (m, 1 H), 1.66 (s, 1.5 H), 1.73 (m, 1 H), 2.85 (m, 1 H), 2.97 (m, 1 H), 3.27 (m, 3 H), 3.68 (m, 2 H), 3.94 (s, 0.5 H), 4.02 (t, 1 H, J = 9.6 Hz), 4.30 (d, 1 H, J = 11.4 Hz), 4.36 (dd, 1 H, J = 6.0 and 12.0 Hz), 4.39 (d, 1 H, J = 11.4 Hz), 4.48 (d, 1 H, J = 11.4 Hz), 4.54 (d, 1 H, J = 11.4 Hz), 4.77 (d, 1 H, J = 12.0 Hz), 4.92 (d, 1 H, J = 10.8 Hz), 4.95 (d, 1 H, J = 12.0 Hz), 7.05−7.51 (m, 15 H, ArH); ^{13}C NMR (150 MHz, C_6D_6) δ 3.3, 20.5, 33.7, 63.6, 69.0, 71.4, 74.2, 74.5, 74.8, 74.84, 75.2, 82.6, 102.0, 127.5, 127.6, 127.7, 127.9, 128.1, 128.2, 128.3, 128.4, 128.5, 138.8, 138.9, 139.5, 170.0. HR-EI-MS m/z $[M]^+$ calcd for $C_{32}H_{37}O_7I_1$ 660.1578, $C_{32}H_{36}{}^2H_1O_7I_1$ 661.1641, $C_{32}H_{34}{}^2H_3O_7I_1$ 663.1767 and $C_{32}H_{33}{}^2H_4O_7I_1$ 664.1830, found 660.1562, 661.1648, 663.1758 and 664.1801 respectively. For the minor product (α-anomer): $[\alpha]^{23}_D$ −4.7 (c 0.3 in $CHCl_3$); IR ν 3031, 2921, 1737, 1345, 1085; ^{1}H NMR (600 MHz, C_6D_6) δ 1.57 (m, 2 H), 1.71 (s, 1.5 H), 2.76 (t, 2 H, J = 6.9 Hz), 3.06 (m, 1 H), 3.49 (m, 1 H), 3.74 (d, 1 H, J = 3.0 Hz), 3.92 (m, 1 H), 3.97 (dd, 1 H, J = 3.0 and 9.6 Hz), 4.17 (t, 1 H, J = 9.0 Hz), 4.41−4.63 (m, 7 H, CH_2Ph), 4.79 (d, 0.5 H, J = 1.2 Hz, H-1), 4.95 (d, 1 H, J = 10.8 Hz, CH_2Ph), 7.03−7.36 (m, 15 H, ArH); ^{13}C NMR (150 MHz, C_6D_6) δ 2.6, 20.6, 33.2, 63.7, 67.1, 71.2, 72.2, 73.1, 75.1, 75.3, 75.5, 80.7, 98.6, 127.5, 127.6, 127.7, 127.9, 128.1, 128.2, 128.3, 128.4, 128.5, 138.8, 138.9, 139.5, 170.0. HR-EI-MS m/z $[M]^+$ calcd for $C_{32}H_{37}O_7I_1$ 660.1578, $C_{32}H_{36}{}^2H_1O_7I_1$ 661.1641, $C_{32}H_{34}{}^2H_3O_7I_1$ 663.1767 and $C_{32}H_{33}{}^2H_4O_7I_1$ 664.1830, found 660.1585, 661.1654, 663.1770 and 664.1830, respectively.

Calculation of the Kinetic Isotope Effect. The ^{1}H NMR spectra of the starting acetates **16**:**17** (1:1), the crude mixture, the β- and α-mannoside products and the internal standard were recorded in C_6D_6 using 600 MHz. For each of these materials, the acetate protons at C6, the anomeric and the internal standard protons were carefully integrated on an expanded region of the desired peak with a standard one pulse sequence. Each spectrum was integrated 10 times and the average value of these integrations was recorded in Table 1 and 2. The α-DKIE of the β-mannoside **19** was determined using the equation KIE = $\ln(1 - F)/\ln[1 - (FR/R_0)]$, where F is the percentage conversion of iodide **18** to the β-mannoside **19** (yield of [**16** + **17**]). R and R_0 are the ratios of the acetate to the anomeric proton integrations in the product **19** and the starting acetates (**16** + **17**) respectively.

KIE of the α-mannoside was determined using the same equation, $\ln(1 - F)/\ln[1 - (FR/R_0)]$, where F is the percentage conversion of the iodide **18** to the α-mannoside **20** (yield of **16** + **17**), and R

TABLE 1. KIEs Measured for the β-Anomer[a]

reaction	KIE	F	R	R_0	S	S_0	N	N_0
β1	1.13	0.493	1.019	1.109	0.415	0.841	0.407	0.758
β2	1.17	0.564	1.000	1.109	0.48	0.849	0.48	0.765
β3	1.16	0.587	1.006	1.108	0.493	0.839	0.49	0.756
β4	1.16	0.444	0.991	1.109	0.377	0.848	0.380	0.764
average	1.155							
STDEV	0.020							

[a] S = ratio of acetate peak of product/internal standard peak. S_0 = ratio of acetate peak of starting material/internal standard peak. R = ratio of acetate peak/anomeric peak in the product. R_0 = ratio of acetate peak/anomeric peak in the starting material. N = ratio of anomeric peak of product/internal standard peak. N_0 = ratio of anomeric peak of starting material/internal standard peak.

TABLE 2. KIEs Measured for the α-Anomer[a]

reaction	KIE	*F*	*R*	R_0	*S*	S_0	*N*	N_0
α1	1.26	0.039	0.878	1.109	0.033	0.841	0.038	0.758
α2	1.13	0.086	0.990	1.109	0.073	0.849	0.074	0.765
α3	1.19	0.07	0.935	1.108	0.066	0.839	0.071	0.756
α4	1.18	0.0487	0.938	1.109	0.041	0.847	0.044	0.763
average	1.19							
STDEV	0.05							

[a] *S* = ratio of acetate peak of product/internal standard peak. S_0 = ratio of acetate peak of starting material/internal standard peak. *R* = ratio of acetate peak/anomeric peak in the product. R_0 = ratio of acetate peak/anomeric peak in the starting material. *N* = ratio of anomeric peak of product/internal standard peak. N_0 = ratio of anomeric peak of starting material/internal standard peak.

and R_0 are the ratios of the acetate to the anomeric protons integrations in the product **20** and the starting acetates (**16** + **17**), respectively.

Acetyl 2,3-Di-*O*-benzyl-4,6-*O*-benzylidine-α/β-D-mannopyranoside (23). To a stirred solution of 2,3-di-*O*-benzyl-4,6-*O*-benzylidine-α-D-mannopyranose **22** (40 mg, 0.09 mmol) in DCM (0.5 mL, 0.18 mmol) was added acetic anhydride (30 μL, 0.32 mmol) followed by triethylamine (0.1 mL, 0.68 mmol) at rt for 4 h. Upon reaction completion, the mixture was quenched with methanol (2 mL) and concentrated in vacuo, and the concentrated residue was subjected to column chromatography (85:15 hexane/ethyl acetate) to afford the title compound (93%, 1:2 α/β) as a colorless syrup. For the β anomer R_f = 0.59 (15% ethyl acetate in toluene): $[\alpha]^{23}_D$ +6.4 (*c* 1.65 in $CHCl_3$); IR ν 2897, 1757, 1370, 1219, 1083; ^{1}H NMR (600 MHz, C_6D_6) δ 1.62 (s, 3 H), 3.17 (m, 1 H), 3.34 (dd, 1 H, *J* = 3.0 and 9.6 Hz), 3.48 (t, 1 H, *J* = 10.2 Hz), 3.56 (d, 1 H, *J* = 3.0 Hz), 4.07 (dd, 1 H, *J* = 4.8 and 10.2 Hz), 4.22 (t, 1 H, *J* = 9.6 Hz), 4.50 (d, 1 H, *J* = 12.6 Hz), 4.73 (d, 1 H, *J* = 12.6 Hz), 4.77 (d, 1 H, *J* = 11.4 Hz), 4.84 (d, 1 H, *J* = 11.4 Hz), 5.14 (s, 1 H), 5.46 (d, 1 H, *J* = 1.2 Hz), 7.06−7.63 (m, 15 H, ArH); ^{13}C NMR (150 MHz, C_6D_6) δ 20.4, 68.3, 68.5, 73.1, 75.7, 77.1, 78.8, 78.9, 93.5, 101.7, 126.7, 127.7, 127.8, 127.9, 128.0, 128.1, 128.2, 128.3, 128.4, 128.5, 128.7, 129.0, 138.6, 139.3, 139.32, 168.4; HR-MALDI *m*/*z* $[M + Na]^+$ calcd for $C_{29}H_{30}NaO_7$ 513.1889, found 513.1780. For the α-anomer, R_f = 0.65 (15% ethyl acetate in toluene): ^{1}H NMR (600 MHz, C_6D_6) δ 1.65 (s, 3 H), 3.73 (t, 1 H, *J* = 10.2 Hz), 3.92 (m, 1 H), 4.17 (m, 2 H), 4.31 (dd, 1 H, *J* = 4.8 and 10.2 Hz), 4.64 (t, 1 H, *J* = 10.0 Hz), 4.72 (d, 1 H, *J* = 12.0 Hz), 4.75 (d, 1 H, *J* = 12.0 Hz), 4.85 (d, 1 H, *J* = 12.0 Hz), 5.00 (d, 1 H, *J* = 12.0 Hz), 5. 46 (s, 1 H), 6.62 (d, 1 H, *J* = 1.2 Hz), 7.23−7.76 (m, 15 H, ArH); ^{13}C NMR (150 MHz, C_6D_6) δ 20.3, 67.0, 68.8, 73.4, 74.0, 76.4, 76.5, 79.3, 93.0, 101.9, 126.7, 127.7, 127.8, 127.9, 128.0, 128.1, 128.2, 128.3, 128.4, 128.5, 128.6, 128.7, 129.0, 138.5, 138.6, 139.3, 168.2; HR-MALDI *m*/*z* $[M + Na]^+$ calcd for $C_{29}H_{30}NaO_7$ 513.1889, found 513.1562.

1-*O*-(3-Iodopropyl)-2,3-di-*O*-benzyl-4,6-*O*-benzylidine-β-D-mannopyranoside (25). To a stirred solution of acetyl 2,3-di-*O*-benzyl-4,6-*O*-benzylidine-α/β-D-mannopyranoside **23** (99 mg, 0.20 mmol) in DCM (1 mL, 0.17 mmol) at 0 °C was added TMSI (31 μL, 2.2 mmol). After 30 min, MgO (16 mg, 0.4 mmol) and trimethylene oxide (20 μL, 0.3 mmol) were added at the same temperature, and then the reaction was stirred at room temperature for 2d. Upon reaction completion, the mixture was diluted with DCM (15 mL) and washed with satd $Na_2S_2O_3$ (2 × 5 mL) and brine (2 × 5 mL). The organic extract was dried (Na_2SO_4), concentrated in vacuo and subjected to column chromatography (hexane/ethyl acetate 90:10) to afford the title compound (65% over two steps) as a colorless syrup: R_f = 0.69 (15% ethyl acetate in toluene); $[\alpha]^{23}_D$ −31.3 (*c* 0.15 in $CHCl_3$); IR ν 2923, 1092; ^{1}H NMR (600 MHz, C_6D_6) δ 1.66 (m, 2 H), 2.86 (m, 1 H), 2.95 (m, 1 H), 3.06 (m, 1 H), 3.19 (m, 1 H), 3.39 (dd, 1 H, *J* = 3.0 and 9.6 Hz), 3.61 (m, 2 H), 3.66 (d, 1 H, *J* = 3.0 Hz), 3.86 (s, 1 H), 4.17 (dd, 1 H, *J* = 4.8 and 10.2 Hz), 4.29 (t, 1 H, *J* = 9.5 Hz), 4.63 (d, 1 H, *J* = 12.6 Hz), 4.78 (d, 1 H, *J* = 12.0 Hz), 4.86 (d, 1 H, *J* = 12.0 Hz), 4.95 (d, 1 H, *J* = 12.0 Hz), 5.25 (s, 1 H) 7.03−7.63 (m, 15 H, ArH); ^{13}C NMR (150 MHz, C_6D_6) δ 3.2, 33.7, 67.9, 68.8, 68.9, 72.6, 75.6, 77.7, 78.4, 79.3, 101.7, 102.4, 126.7, 127.8, 127.9, 127.94, 128.0, 128.1, 128.2, 128.3, 128.4, 128.43, 128.5, 128.6, 128.9, 138.7, 139.5, 139.6; HR-MADI $[M + Na]^+$ *m*/*z* calcd for $C_{30}H_{33}INaO_6$ 639.1220, found 639.1190.

Computational Methods

The structures reported herein (images generated with Ball & Stick 4.0a12[50]) were optimized in the gas phase using the Gaussian 03 suite of programs[51] utilizing the Becke three-parameter hybrid functional combined with the Lee−Yang−Parr correlation functional.[52−55] The 6-31+G(d,p) basis set was used for C, O, and H atoms and the LANL2DZ basis set[56] was used for I atoms. This level of theory is referred to throughout as B3LYP/6-31+G(d,p): LANL2DZ.

An exhaustive search of conformational space was not practical at this level of theory, so the substituents on the mannose oxygens were initially oriented in what appeared to be the least sterically crowded directions and then allowed to relax during the geometry optimization procedure; the same initial orientations were used for all structures.

SCHEME 7. Series of Partially Constrained Optimizations Leading to Structure E[a]

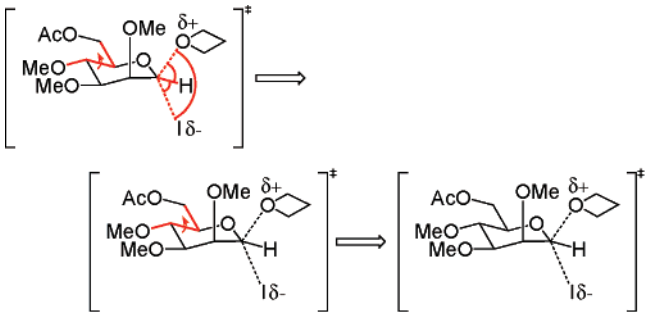

[a] An analogous procedure was used to locate structure **F**. Bolded red bonds and lines indicate a constrained bond length, angle, or dihedral angle during the optimization procedure.

Geometries from structures **C** and **D** (Figure 3) were used as starting points for a series of constrained optimizations (Scheme 7) aimed at finding analogous conformers of **A** and **B**. The methylene bridge was removed and replaced with methyl and

(50) Müller, N.; Falk, A.Ball & Stick 4.0a12, Molecular Graphics Software for MacOS, Johannes Kepler University Linz, 2000.
(51) Frisch, M. J.; Trucks, G. W.; Schlegel, H. B.; Scuseria, G. E.; Robb, M. A.; Cheeseman, J. R.; Montgomery, J. A. Jr.; Vreven, T. K. K. N.; Burant, J. C.; Millam, J. M.; Iyengar, S. S.; Tomasi, J.; Barone, V.; Mennucci, B.; Cossi, M.; Scalmani, G.; Rega, N.; Petersson, G. A.; Nakatsuji, H.; Hada, M.; Ehara, M.; Toyota, K.; Fukuda, R.; Hasegawa, J.; Ishida, M.; Nakajima, T.; Honda, Y.; Kitao, O.; Nakai, H.; Klene, M. L. X.; Knox, J. E.; Hratchian, H. P.; Cross, J. B.; Adamo, C.; Jaramillo, J.; Gomperts, R.; Stratmann, R. E.; Yazyev, O.; Austin, A. J.; Cammi, R.; Pomelli, C.; Ochterski, J. W.; Ayala, P. Y.; Morokuma, K.; Voth, G. A.; Salvador, P.; Dannenberg, J. J.; Zakrzewski, V. G.; Dapprich, S.; Daniels, A. D.; Strain, M. C.; Farkas, O.; Malick, D. K.; Rabuck, A. D.; Raghavachari, K.; Foresman, J. B.; Ortiz, J. V.; Cui, Q.; Baboul, A. G.; Clifford, S.; Cioslowski, J.; Stefanov, B. B.; Liu, G.; Liashenko, A.; Piskorz, P.; Komaromi, I.; Martin, R. L.; Fox, D. J.; Keith, T.; Al-Laham, M. A.; Peng, C. Y.; Nanayakkara, A.; Challacombe, M.; Gill, P. M. W.; Johnson, B.; Chen, W.; Wong, M. W.; Gonzalez, C.; Pople, J. A. *Gaussian 03*, Revision B.04: Gaussian, Inc.: Pittsburgh PA 2003.
(52) Becke, A. D. *J. Chem. Phys.* **1993**, *98*, 5648−5652.
(53) Stephens, P. J.; Devlin, F. J.; Chabalowski, C. F.; Frisch, M. J. *J. Phys. Chem.* **1994**, *98*, 11623−11627.
(54) Lee, C.; Yang, W.; Parr, R. G. *Phys. Rev.* **1988**, 785−789.
(55) Becke, A. D. *J. Chem. Phys.* **1993**, *98*, 1372−1377.
(56) Hay, P. J.; Wadt, W. R. *J. Chem. Phys.* **1985**, *82*, 270−283.

acetate groups and an optimization was performed allowing everything to relax with the exception of the indicated O−C−C−C dihedral angle and indicated bonds and angles around the anomeric carbon. The resulting geometry was then allowed to relax with the exception of the indicated O−C−C−C dihedral angle. Finally all constraints were removed, and the atoms were allowed to relax to the transition structures shown in Figure 4.

Saddle points **A** and **B** were connected to reactant complexes using intrinsic reaction coordinate[57,58] searches (see the Supporting Information for details). Energy values reported are in kcal/mol and zero-point corrected (with no scaling factor applied). Vibrational frequency analysis on the stationary points provided the frequencies for the KIE calculations which were processed with QUIVER, a program[59] employing the method introduced by Bigeleisen and Mayer.[60] Tunneling corrections, while minimal, were applied using the one-dimensional infinite parabolic barrier model.[61,62]

Acknowledgment. National Science Foundation CHE-0196482, NSF CRIF program (CHE-9808 183), NSF Grant OSTI 97-24412, and NIH Grant RR11973 provided funding for the NMR spectrometers used in this project. D.J.T. and D.W. gratefully acknowledge support from UC Davis and the American Chemical Society's Petroleum Research Fund and thank Prof. Dan Singleton for information on processing the computational KIE data.

Supporting Information Available: NMR spectra and additional details on computations. This material is available free of charge via the Internet at http://pubs.acs.org.

JO070229Y

(57) Gonzalez, C.; Schlegel, H. B. *J. Phys. Chem.* **1990**, *94*, 5523−5527.
(58) Fukui, K. *Acc. Chem. Res.* **1981**, *14*, 363−368.
(59) Saunders, W.; Laidig, K. E.; Wolfsberg, M. *J. Am. Chem. Soc.* **1989**, *111*, 8989−8994.
(60) Bigeleisen, J.; Mayer, M. G. *J. Chem. Phys.* **1947**, *15*, 261−267.
(61) Bell, R. P. *Chem. Soc. Rev.* **1974**, *3*, 513−544.
(62) Bell, R. P. *The Tunnel Effect in Chemistry*; Chapman and Hall: London, 1980; pp 60−63.